OVERCOMING OF BARRIER BETWEEN CAD AND CFD BY MODIFIED FINITE VOLUME METHOD

Andrey Aksenov
Alexander Dyadkin
Institute for Computer Aided Design of RAS
19/18, ul. 2-ya Brestskaya, Moscow, Russia, 123056
E-mail: FlowVision@glas.apc.org

Victor Pokhilko
Institute for Mathematical Modeling of RAS
4a Miusskaya sq,
Moscow, Russia, 125047
E-mail: FlowVision@glas.apc.org

ABSTRACT An advanced finite-volume method (method of modified finite volumes) for numerical simulation of flows in industrial applications and its implementation in code ***FlowVision*** is proposed. The method is based on non-staggered Cartesian grid with adaptive local refinement and a subgrid geometry resolution method for description of curvilinear complex boundaries. Semi-Lagrange approach for solution of convective transport equation and splitting algorithm for solution of Navier-Stokes equations are presented.

Opportunity of solution of real industrial problems by the method of modified finite volumes is estimated. Geometry of computational domain is specified by CAD system and is imported by ***FlowVision*** through VRML or STL file.

Two different problems was investigated by the proposed method. The first problem is an aquaplane of car tire on road with water layer, the second -- a combustion of methane in air by low NOx burner of power station boiler.

INTRODUCTION The creation of any technical object passes a tedious path from idea, via a lot of experiments, up to object functioning in compliance with the initial idea. Use of technology of computer aided design (CAD) is called to reduce the time of creation. The final goal of CAD is to have line-up: Idea - CAD - Manufacture - Object. To achieve this goal the CAD systems have to predict properties of the projected object. Engineering analysis systems perform these predictions. They include, for example, analysis of deformations-strains and interaction with environment. Use of industrial computational fluid dynamics (ICFD) allows to simulate an interaction between object and fluids.

To integrate ICFD in CAD a barrier between them must be overcome. The barrier consists in different geometrical objects that are operated by CAD systems and methods of computational fluid dynamics. Geometry is specified as surfaces in CAD, but ICFD methods need volume grid generation between these surfaces.

There are some grid types that differ each other by grid cell geometry. Nowadays grids with tetrahedron or hexagon cells are most widely used.

Generation methods for unstructured tetrahedron grid are well known and make use of finite element analysis of a pressure strain state of technical objects. But accuracy and speed of flow simulation on tetrahedron grid are not high in comparison with hexagon grids. However automatic generation of hexagon grid is a great problem now.

ICFD application is characterized by a large difference between spatial and temporal scales, complex and arbitrary object shape and a wide range of physical and chemical phenomena. So it is preferably utilized adaptive grids to resolve these singularities. On the other hand it has meaning only for fast grid adaptation methods.

A method of modified finite volumes (MMFV) for fluid flow simulation is described in this paper. The method is based on Cartesian adaptive locally refined grid (ALRG) coupled with subgrid geometry resolution method (SGRM) for description of curvilinear surfaces. Object shape is represented by a set of plane facets. Almost all CAD systems generate facets from their inner representation of geometry model, so MMFV can be used for the integration with CAD systems.

Semi-Lagrange approach for solution of convective transport equation is used in MMFV. This approach allows to calculate a flow in computational domain with moving boundaries and to solve problems of interaction between fluid and structure.

The method of modified finite volumes is being implemented by the authors in CFD code ***FlowVision*** (Aksenov, Gudzovsky, 1993; Aksenov et al., 1996a; Aksenov et al., 1996b). Object oriented technology was used for creation of the code that easily permits to adapt code for different ICFD problems. ***FlowVision*** works under Windows'95/NT operating system, has user friendly interface for specifying task parameters and results analyzing. Interface between some CAD systems (SolidWorks and ZCAD) was implemented.

In this paper we present the main features of the method of modified finite volumes and its application for two different problems -- simulation of car tire aquaplane and gas combustion by power station burner. Goal of the investigation is to estimate opportunity of solution of real industrial problems by the method and opportunity of use of geometrical information from CAD system by CFD code.

NOMENCLATURE

D - the sum of non-convective terms in Navier-Stokes equations.
P - pressure,
V - fluid velocity,
V_j^i - volume Ω_j^i at the beginning of the time step,
V_i - volume of the i-th grid cell,
t - time,
f - scalar variable,
$\hat{f}$ - auxiliary variable,
f_i - average value of the variable over i-th grid cell,
f^* - reconstructed function,
Ω - volume that moves with the fluid,
Ω_i - volume Ω from i-th cell at the end of the time step,
Ω_i^j – intersection of Ω_i and V_j
ρ - fluid density,
τ - time step,

METHOD OF MODIFIED FINITE-VOLUMES

Subgrid Geometry Resolution Method An adaptive locally refined rectangular grid is introduced in computational domain. The grid is a collection of grids of different levels with rectangular cells. A grid of first level is an ordinary structured grid. Each cell of the grid can be subdivided (when adaptation occurs) by eight cells of a higher level grid and these cells can be subdivided too. The grid information stores as octree in C++ database.

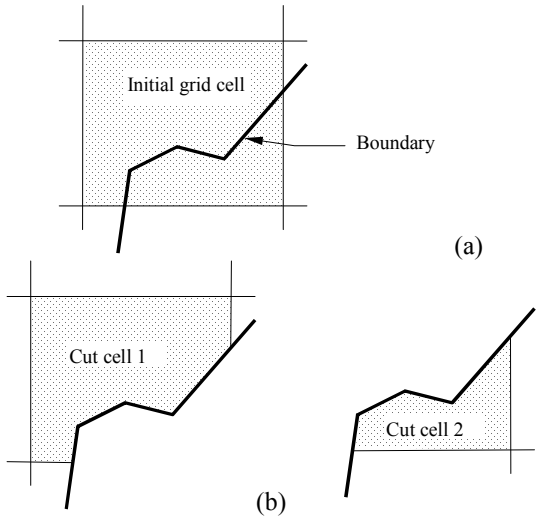

Figure 1. Initial grid cell (a) disjoined by facet surface on modified finite volumes (b)

Let curvilinear boundary be represented by a set of plane facets. A subgrid resolution method is used 'to fit' Cartesian grid to boundaries and to describe accurately boundary conditions. This method is developed in (Aksenov et al., 1996b). An algorithm of this method consists in four steps. At the first step the grid cells intersected by the facets are found (Fig. 1a). At the second step initial "parent" rectangular cell is cut off by facet surfaces. The parent cell is disjoined on some volumes of complex shape bounded by facets and grid cell faces (Fig. 1b). At the third step all geometrical information which is necessary for approximation of governing equations, is determined; that is volume of a new cell, squares of boundaries, distances from boundaries to a mass-center of the cell and its neighbors. At the fourth step very small cells (those volumes are less then 0.2 volume of parent cell) are removed and their boundaries are transmitted to neighboring cells.

Solution of the Transport Equation In computational hydrodynamics a most difficult problem is a solution of convective transport equation. Consider the solution of this equation by method of modified finite volumes.

Let us initially enumerate all finite volumes by index i. Introduce average value f_i of some variable f (component of speed, concentration, temperature and etc.) over a grid cell V_i during time step $\tau = t^{n+1}-t^n$

$$f_i^n = \int_{V_i} f(\mathbf{x},t^n)dV \qquad (1)$$

Consider approximate reconstruction operator $R(V_i, V_{j1}, V_{j2}, ...)$ of $f(\mathbf{x},t)$ from averages in V_i and surrounding this cell neighboring cells V_j

$$f_i \xrightarrow{R} f^*(\mathbf{x},t) \qquad (2)$$

where $f^*(\mathbf{x},t)$ is a reconstructed function. The reconstruction R should have property that average of f^* equals again f_i

$$f_i^n = \int_{V_i} f^*(\mathbf{x},t^n)dV \qquad (3)$$

Different types of reconstruction operator were described in (Aksenov et al, 1996b; Aksenov et al, 1993).

One can write equation for pure convective transport in Lagrange form as

$$\frac{df}{dt} = 0$$

Introduce a volume $\Omega(t)$ moving with the fluid. Volume Ω coincides with V_i at the beginning of the time step

$$\Omega(t^n) \equiv V_i .$$

Designate the volume Ω at the end of the time step as

$$\Omega(t^{n+1}) \equiv \Omega_i.$$

Integration of the transport equation over Ω results in

$$\int_{\Omega_i} f(\mathbf{x}, t^{n+1})dV - \int_{V_i} f(\mathbf{x}, t^n)dV = \int_{\tau}\int_{S_\Omega} DdSdt + \int_{\tau}\int_{S_w} GdSdt \quad (4)$$

where S_Ω is a fluid boundary of Ω, S_w is a rigid boundary with boundary conditions, D and G are diffusion fluxes through S_Ω and S_w respectively.

To derive numerical scheme for calculation of f_i^{n+1} we split equation (4) onto convective and non-convective parts and approximate them as follows

$$\int_{\Omega_i} \hat{f}(\mathbf{x})dV = \int_{V_i} f^*(\mathbf{x}, t^n)dV \quad (5)$$

$$\int_{\Omega_i} f(\mathbf{x}, t^{n+1})dV = \int_{\Omega_i} \hat{f}(\mathbf{x})dV + \tau\left(\int_{S_{\Omega_i}} DdS + \int_{S_w} GdS\right)_{t=t^{n+1}} \quad (6)$$

Here $\hat{f}$ is intermediate field, variables $f(\mathbf{x},t)$ were replaced by its reconstructed functions (2).

One can modify (5) to find averages of $\hat{f}$ over the grid cells. The equation (5) shows a transfer of variable f from the cells to their neighbors. Each i-th cell is surrounded by donor neighbor cells (value of f transfers from they to i-th cell) and acceptor neighbors (value of f transfers from the cell to neighbors). Designate an intersection of volume Ω_i from i-th cell with j-th cell V_j (Fig. 2) as

$$\Omega_i^j = \Omega_i \cap V_j$$

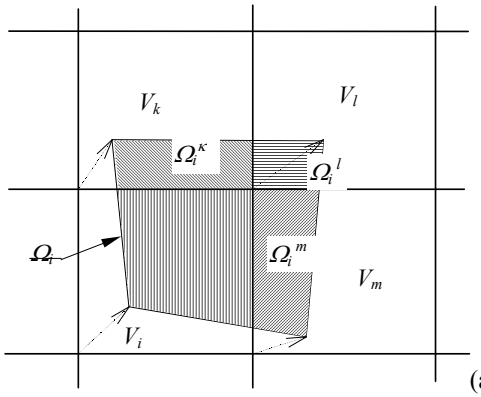

(a)

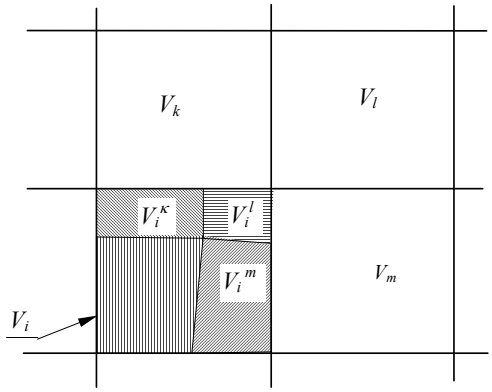

(b)

Figure 2. Subdivision of the volume Ω (a) and corresponding subdivision of the cell (b)

If j-th neighbor is acceptor then $\Omega^j{}_i \neq 0$, if j-th neighbor is donor then $\Omega^j{}_i = 0$, but intersection of its own moving volume is not zero: $\Omega^i{}_j \neq 0$. Covering the i-th cell by Ω-volumes we find $\hat{f}_i$

$$\hat{f}_i = \frac{1}{V_i}\left(\int_{\Omega_i} f(\mathbf{x})dV + \sum_j \int_{\Omega_j^i} f(\mathbf{x})dV - \sum_k \int_{\Omega_i^k} f(\mathbf{x})dV\right) \quad (7)$$

Here index j designates donor neighbors, k -- acceptor neighbors. Each volume $\Omega^i{}_j$ coincides before beginning of its motion with corresponding subvolume V^i_j

$$V^i_j = \Omega^i{}_j\,(t = t^n) \quad (8)$$

Now we can write final expression for $\hat{f}_i$ using equations (5), (7) and definitions (3), (8)

$$\hat{f}_i = f_i^n + \frac{1}{V_i}\left(\sum_j \int_{V_j^i} f^*(\mathbf{x}, t^{n+1})dV - \sum_k \int_{V_i^k} f^*(\mathbf{x}, t^{n+1})dV\right) \quad (9)$$

The volume of integration in (6) is changed on V_i to find f_i^{n+1}. We get

$$f_i^{n+1}V_i = \int_{V_i} \hat{f}^*(\mathbf{x})dV + \tau\left(\int_{S_{V_i}} DdS + \int_{S_{w,v}} GdS\right)_{t=t^{n+1}} \quad (10)$$

where the definition of f_i^{n+1} (1) was used to write the left hand side of (6).

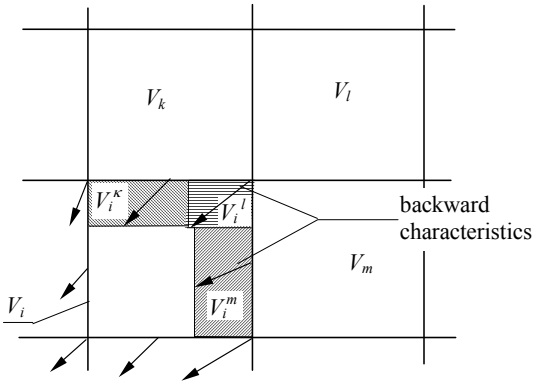

Figure 3. Approximation of the cell subdivision

To calculate equation (8) a fast method of constructing of V_i^j volumes is required. To simplify integration it is desirable that these volumes were rectangular. The next method is offered in this paper.

Backward characteristics initially are let off cell vertexes, edges and faces (Fig. 3). Then the rectangular subvolumes V_i^j are built for characteristics going inside the cell. Each subvolume is built by intrusion of its corresponding geometrical object (vertex, edge and face) inside cell along characteristic. Vertex characteristic-based subvolumes are built first. The vertex-based subvolumes are built by intrusion of cell vertex inside cell. Then edge-based subvolumes are built taking into account existing vertex-based subvolumes. Vectors of this intrusion are defined by orthogonal components of edge characteristic to cell edges. The face-based volumes are built latest taking into account all early built subvolumes. The intrusion vectors are defined by orthogonal components of face characteristic to cell faces.

Solution of Navier-Stokes Equations Solution algorithm of Navier-Stokes equations was developed for two types of fluid flows -- incompressible and weak compressible flow.

Continuity equation written in Lagrange integral form for volume Ω moving with fluid during τ is

$$\int_{\Omega_i} \rho dV = \int_{V_i} \rho dV \tag{11}$$

Here ρ is a fluid density. Another form of this equation is used for compressible flow

$$\int_{V_i} \rho^{n+1} dV = \int_{V_i} \rho^{n} dV - N \tag{12}$$

where N designates a term in continuity equation

$$N = \tau \int_{V_i} \nabla \rho \mathbf{V} dV \equiv \tau \int_{S_{V_i}} \rho \mathbf{V} dS \tag{13}$$

Here $\mathbf{V}$ is fluid velocity field. For incompressible fluid (for tire aquaplane modeling) density is calculated from convective transport equation (11). For weak compressible fluid (flow with combustion) the density is calculated from equation of state, so all volume integrals in equation (12) are known and N can be defined directly from it.

Write Navier-Stokes equation in Lagrange form as

$$\int_{\Omega_i} \mathbf{V} dV - \int_{V_i} \mathbf{V} dV = -\iint_{\tau,\,\Omega} \frac{\nabla P}{\rho} dV dt + \mathbf{D} \tag{14}$$

Here P is pressure, $\mathbf{D}$ is the sum of viscosity stress, gravity force and other non-convective terms in Navier-Stokes equations.

The pressure term in equation (14) is a volume integral averaged over time step. This term is approximated by pressure integral over volume Ω_i at the end of time step. Adding and subtracting the same term for pressure but at n time step we get

$$\int_{\Omega_i} \mathbf{V}^{n+1} dV - \int_{V_i} \mathbf{V}^{n} dV \cong$$
$$-\tau \{ \int_{\Omega_i} \frac{\nabla P^{n+1}}{\rho^{n+1}} dV - \int_{\Omega_i} \frac{\nabla P^{n}}{\rho^{n}} dV + \int_{\Omega_i} \frac{\nabla P^{n}}{\rho^{n}} dV \} + \mathbf{D} \tag{15}$$

Following an ordinary procedure of solution of Navier-Stokes equation we can split equation (15) into two parts by introducing intermediate velocity field $\tilde{\mathbf{V}}_i$

$$\int_{\Omega_i} \tilde{\mathbf{V}} dV - \int_{V_i} \mathbf{V}^{n} dV = -\tau \int_{\Omega_i} \frac{\nabla P^{n}}{\rho^{n}} dV + \mathbf{D} \tag{16}$$

$$\int_{\Omega_i} \mathbf{V}^{n+1} dV - \int_{\Omega_i} \tilde{\mathbf{V}} dV = -\tau \{ \int_{\Omega_i} \frac{\nabla P^{n+1}}{\rho^{n+1}} dV - \int_{\Omega_i} \frac{\nabla P^{n}}{\rho^{n}} dV \} \tag{17}$$

One can see that equation (16) is the transport equation of type (4) and this equation can be solved by scheme (9,10) to find $\tilde{\mathbf{V}}_i$ field.

Derive equation for determination of pressure field at next time step P^{n+1}. A differential analog of (17) is

$$\mathbf{V}^{n+1} - \tilde{\mathbf{V}} = -\tau \{ \frac{\nabla P^{n+1}}{\rho^{n+1}} - \frac{\nabla P^{n}}{\rho^{n}} \} \tag{18}$$

Use condition $\nabla \mathbf{V}^{n+1} = 0$ for incompressible fluid, then apply divergence operation and Gauss theorem to (18) we get equation for calculation of P^{n+1}

$$\int_{S_{v_i}} \tilde{\mathbf{V}} d\mathbf{S} = -\tau \{ \int_{S_{v_i}} \frac{\nabla P^{n+1}}{\rho^{n+1}} d\mathbf{S} - \int_{S_{v_i}} \frac{\nabla P^{n}}{\rho^{n}} d\mathbf{S} \} \tag{19a}$$

Equation (12) is used for compressible flow and we get

$$\int_{V_i} \nabla(\rho^{n+1}\mathbf{V}^{n+1})dV \equiv N = \int_{S_{V_i}} \rho^{n+1}\{\widetilde{\mathbf{V}}dV - \tau(\frac{\nabla P^{n+1}}{\rho^{n+1}} - \frac{\nabla P^{n}}{\rho^{n}})\}dS \quad (19b)$$

A finite-difference form of pressure equations (19a),(19b) is a discrete Laplace equation.

To calculate $\mathbf{V}^{n+1}$ we have to simply substitute the definition of averages in the cell (3) in (18)

$$\mathbf{V}_i^{n+1} - \widetilde{\mathbf{V}}_i = -\tau\{\int_{V_i} \frac{\nabla P^{n+1}}{\rho^{n+1}}dV - \int_{V_i} \frac{\nabla P^{n}}{\rho^{n}}dV\} \quad (20)$$

Therefore equations (11-13) are solved the follows algorithm.

1. Put n=0 and some guess for $\mathbf{V}^0$, ρ^0 and P^0.
2. For incompressible flow: Transport equation (11) is solved and ρ^{n+1} is found. For compressible flow: from (12) N is calculated
3. Transport equation (16) is solved and intermediate velocity field $\widetilde{\mathbf{V}}$ is found.
4. The pressure field at (n+1)-th time step is calculated from corresponding Laplace equation (19) by iterative methods (conjugate gradients or successive relaxation methods).
5. Afterward velocity averages over finite volume $\mathbf{V}_i^{n+1}$ are found from (20).
6. Put n=(n+1) if convergence is not reached and go to step 2.

Note non-staggered grids have well-known pressure field oscillations (Patankar, 1980). These oscillations we suppress by correction of equation (19). A difference between 2nd and 4th order approximation of pressure term is introduced in (19a), (19b) according to Armfield (1991).

RESULTS

Car Tire Aquaplane The solution of aquaplane problem was performed for rigid rotated car tire. Influence of protector pattern was investigated on tire lift. Analogous task was solved by finite-element analysis software (Zmindak, Grajciar, 1997). In this solution a body-fitted grid was used. Use of this type of grid does not allow to simulate flow around tire with zero gap between tire and road, but allows simply to take into account a deformation of car tire.

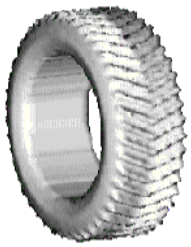

Figure 4. Tire model with inclined channels of treads.

There are two different tasks with essential different mathematical models in aquaplane problem. The first task is flow simulation around car tire, the second -- tire deformation. More accurate and suitable approach for the first task solution is finite-volume method in Euler description, for the second task – finite-element method in Lagrange description. Nowadays use of homogeneous methods for solution of conjugate problems is considered preferable. Use of method such as the method of modified finite volumes, which compatible through the same boundary description with finite-element methods, allows to apply each method in its own area of advantages.

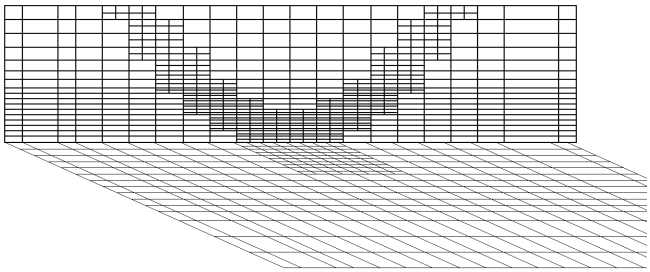

Figure 5. Grid adaptation for tire geometry

Water and air flow around aquaplaning car tire is governed by a system of equations for incompressible fluid which includes continuity and Navier-Stokes equations. Equations are solved in coordinate system moving with the tire. Tire rotates in computational domain with speed corresponding to car velocity. Computational domain was bounded a box with dimension 1.5 m along car motion, 0.1 m in height, 0.8 m along tire axis.

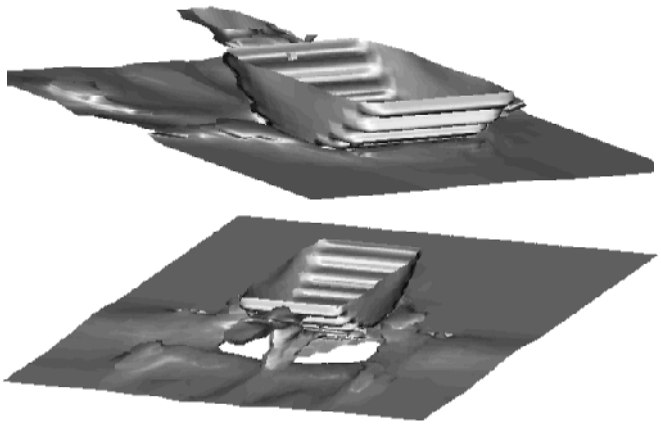

Figure 6. Water surface around the tire with zero inclined channels.

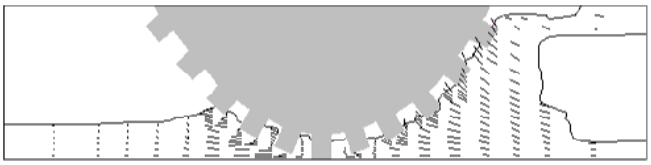

Figure 7. Distribution of water velocity in vertical symmetry plane.

Numerical simulation of water flows around tire model (Fig. 4) was performed. Calculation was made for tire with radius equals to 33 cm (13 in). The tread of 20 cm wide was specified by channels inclined to tire axis. Depth of the channels and the water layer on road were equal to 2 cm. All calculation was made for car speed 20 m/s (76 km/h). Grid was adapted to the tread geometry (Fig. 5).

Water surface disturbed by car tire is shown in Fig. 6. Water surface was reconstructed from density field as isosurface of a density with level equals 700 kg/m^3. One can see the two waves on the water surface -- bow and stern waves. The water jet uploads directly behind the tire and the collapse of the water layer behind the jet occurs.

Velocity distribution and water surface in different planes is shown in Fig. 7 and Fig. 8. Velocity is represented in coordinate system linked with road. One can see that water is extruded under and before the tire, water behind the tire moves to tire. The water has no time to fill in channels of a tire protector and the channels partially are filled by an air. It reduces an effectiveness of water removing from under a tire and results in increasing lifting force.

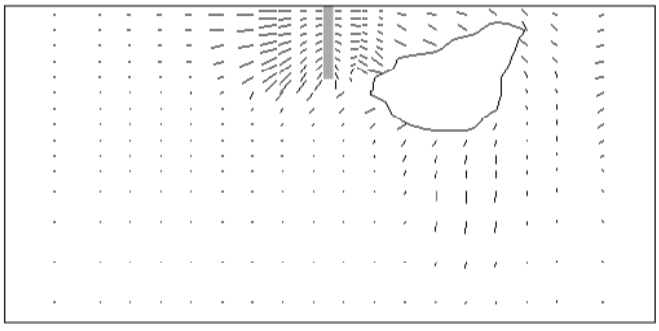

(a)

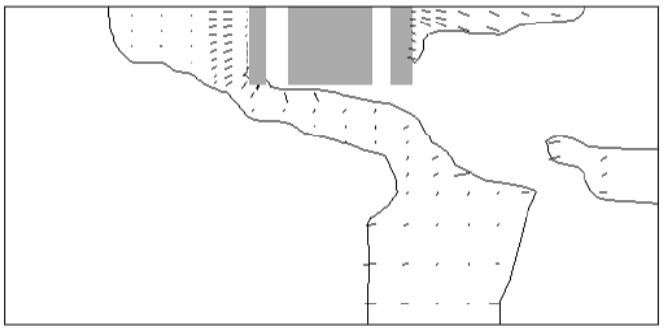

(b)

Figure 8. Distribution of water velocity in horizontal plane at distance from road equals (a) 1 mm, (b) 21 mm.

Gas combustion in burner A two-stage methane combustion is a most effective method for reduction of nitrogen oxide emission. A special burner is projected to realize this process. A numerical simulation of this burner is presented.

Fuel mixture flows by two concentric channels in this burner. There are a strong swirling flow of premixed fuel mixture in internal channel and a straight stream of a pure air in external one.

Mathematical model of physical and chemical processes in burner is based on conservation law of mass, energy and impulse. For description of turbulent transfer we used "standard" Launder-Spalding k-ε model with modifications of ε - equation near burner axis to describe a strong swirling flow. The methane combustion in air is described by one-stage model (Volkov, Kudriavtsev , 1979).

Gas flow simulation in the burner is carried out with and without methane combustion. Because of strong swirling flow a vortex breakdown takes place on burner axis. There is a region of a backward flow for about 2-3 burner diameter D for cold flow (Fig. 9a). In combustion case the backward flow region reduces up to 0.1D for flow with combustion (Fig. 9b). The backward flow is at the flame front and has a role of flame stabilizer.

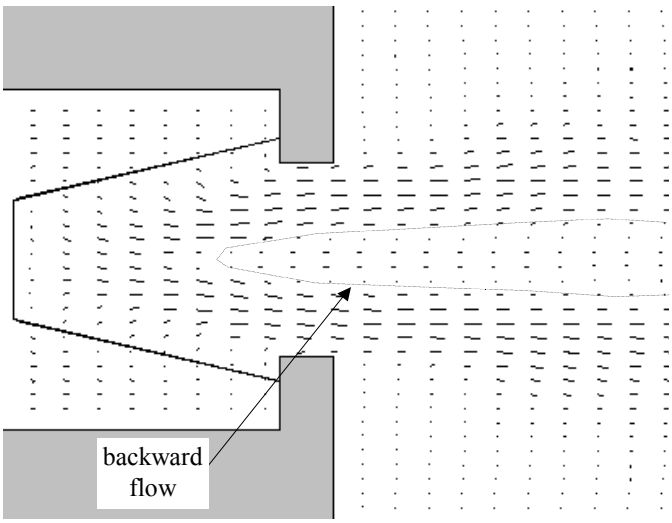

(a)

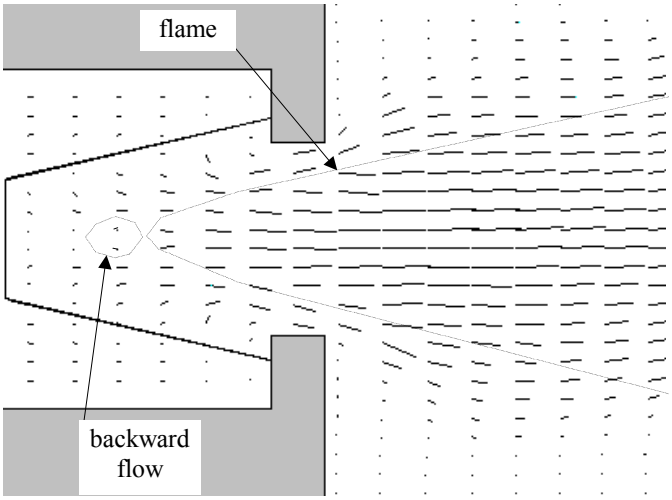

(b)

Figure 9 Distribution of gas velocity in burner and scheme of gas flow, (a) without combustion, (b) with combustion

The methane combustion modeling is shown in Fig. 10. Results are represented by a flame luminescence that is simulated by the rate of fuel decrease. A test work of real burner is shown in Fig. 11 for comparison. The comparison between computational data and real data indicates on an adequacy of constructed combustion model and numerical method.

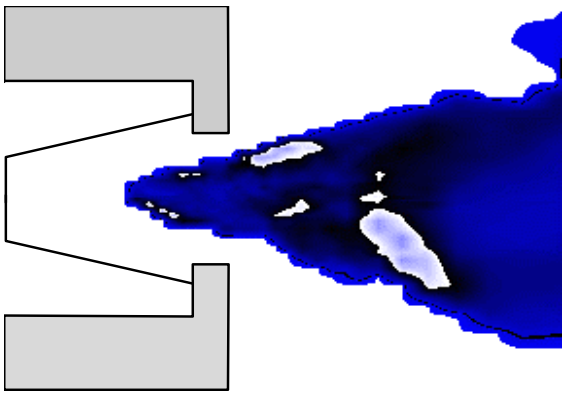

Figure 10. Flame visualization by rate of fuel decrease.

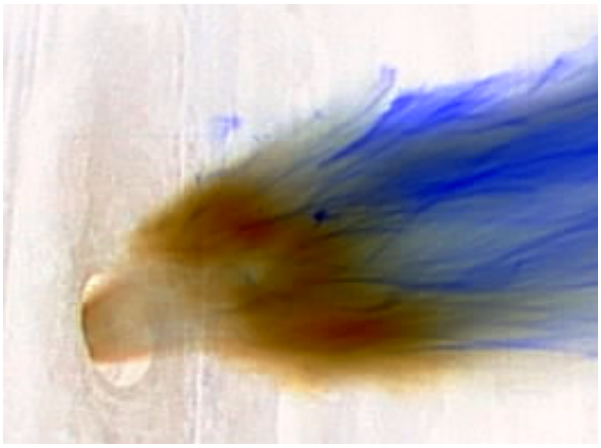

Figure 11. Combustion of methane by the burner in power station boiler (experiment)

CONCLUSION Method of modified finite volumes for solution of hydrodynamic equations is presented. The method uses an adaptive grid with rectangular cells. Boundary conditions is approximated by subgrid geometry resolution method. Semi-Lagrange method is used for solution of convective transport equation. Splitting algorithm is described for solution of Navier-Stokes equation.

Two different problems was investigated by the proposed method. The first problem is aquaplane of car tire on road with water layer, the second -- a combustion of methane by low NOx burner of power station boiler. Geometry of computational domain was specified by SolidWorks CAD system. Geometrical information from SolidWorks is imported by ***FlowVision*** code through facet representation.

The methane combustion in high swirling flow produced by burner was performed. Gas flow simulation in the burner is carried out with and without combustion. The zone of backward

flow on burner axis is found. When combustion occurs the zone is shifted before flame and its size decreases in comparison with flow without combustion. This fact was confirmed by experiments (Tishin, 1997).

Thus opportunity of solution of real industrial problems by the method of modified finite volumes was estimated. Opportunity of use of geometrical information from CAD system by CFD code is shown on an example of solution of two problems.

ACKNOWLEDGMENT This work is supported by RFBR, grant 98-01-00484. The authors express thanks to A. Gudzovsky, T. Luniewski, S. Kursakov and A. Tishin for attention to this work.

REFERENCES

Volkov E.P., Kudriavtsev N.Yu., 1979, "Modeling of nitrogen oxides forming in turbulent diffusive torch", Engineering Physical Journal, V.56, N 6, pp. 775-794.

Patankar S., 1980, "Numerical heat transfer and fluid flow", Himisphere Publishing Corporation, New York.

Armfield S.W., 1991, "Finite Difference Solutions of the Navier-Stokes Equations on Staggered and Non-Staggered Grids", 1-17, Computers Fluids, 20, N 1.

Aksenov, A.A., Gudzovsky, A.V., 1993, "The software ***FlowVision*** for study of air flows, heat and mass transfer by numerical modelling methods", 31-35, in Proc. of the Third Forum of Association of Engineers for Heating, Ventilation, Air-Conditioning, Heat Supply and Building Thermal Physics, 22-25 Aug. 1993, Moscow (in Russian).

Aksenov A.A., Gudzovsky A.V., Serebrov A.A., 1993, "Electrohydrodynamic Instability of Fluid Jet in Microgravity", 19-24, in Proc. of 5th Int. Symposium on Computational Fluid Dynamics (ISCFD), Aug. 31 - Sept. 3, 1993, Sendai, Japan, Japan Society of Computational Fluid Dynamics, Vol.1, 1993.

Aksenov A.A., Gudzovsky A.V., Dyadkin A.A., Tishin A.P., 1996a, "Gaz mixing of Low Head Jet in Crossflow", 67-74, Izvestia of Russian Academy of Sciences, Mechanics of Fluids and Gas, 3 (in Russian).

Aksenov A.A., Dyadkin A.A., Gudzovsky A.V., 1996b, "Numerical Simulation of Car Tire Aquaplaning". Computational Fluid Dynamics '96, J.-A. Desideri, C.Hirsch, P.Le Tallec, M.Pandolfi, J.Periaux edts, John Wiley&Sons, pp. 815-820.

Zmindak M., Grajciar I., 1997, "Simulation of the Aquaplane Problem", Computer & Strucures, Vol. 64, No. 5/6, pp. 1155-1164.

Tishin A.P., 1997, Private communication.